

Article

# Seven-Grooved-Rod, Side-Pumping Concept for Highly Efficient TEM<sub>00</sub>-Mode Solar Laser Emission through Fresnel Lenses

Hugo Costa , Dawei Liang \* , Joana Almeida , Miguel Catela , Dário Garcia , Bruno D. Tibúrcio   
and Cláudia R. Vistas 

Centre of Physics and Technological Research, Physics Department, NOVA School of Science and Technology, 2829-516 Caparica, Portugal

\* Correspondence: dl@fct.unl.pt

**Abstract:** Low-cost, lightweight, and easily available Fresnel lenses are a more alluring choice for solar laser power production, when compared to the costly and complex heliostat-parabolic mirror systems. Therefore, a seven-rod solar laser head was designed and numerically studied to enhance the efficiency in TEM<sub>00</sub>-mode laser power production, employing six Fresnel lenses with 10 m<sup>2</sup> total collection area for collection and concentration of sunlight. Six folding mirrors redirected the solar rays towards the laser head, composed of six fused silica aspheric lenses and rectangular compound parabolic concentrators paired together for further concentration, and a cylindrical cavity, in which seven Nd:YAG rods were mounted and side-pumped. With conventional rods, total TEM<sub>00</sub>-mode laser power reached 139.89 W, which is equivalent to 13.99 W/m<sup>2</sup> collection efficiency and 1.47% solar-to-TEM<sub>00</sub>-mode laser power conversion efficiency. More importantly, by implementing rods with grooved sidewalls, the total laser power was increased to 153.29 W, corresponding to 15.33 W/m<sup>2</sup> collection and 1.61% conversion efficiencies. The side-pumping configuration and the good thermal performance may ensure that the seven-grooved-rod system has better scalability than other previously proposed schemes.

**Keywords:** Fresnel lens; grooved rod; Nd:YAG; solar laser; TEM<sub>00</sub>-mode



**Citation:** Costa, H.; Liang, D.; Almeida, J.; Catela, M.; Garcia, D.; Tibúrcio, B.D.; Vistas, C.R. Seven-Grooved-Rod, Side-Pumping Concept for Highly Efficient TEM<sub>00</sub>-Mode Solar Laser Emission through Fresnel Lenses. *Photonics* **2023**, *10*, 620. <https://doi.org/10.3390/photonics10060620>

Received: 27 March 2023

Revised: 22 May 2023

Accepted: 24 May 2023

Published: 26 May 2023



**Copyright:** © 2023 by the authors. Licensee MDPI, Basel, Switzerland. This article is an open access article distributed under the terms and conditions of the Creative Commons Attribution (CC BY) license (<https://creativecommons.org/licenses/by/4.0/>).

## 1. Introduction

The global energy crisis triggered an increasing interest in the adoption of renewable power, potentially making it surpass coal as the predominant source of electricity production in the near future, while helping to limit global warming to 1.5 °C [1]. Amid a multitude of renewable energy resources, solar is one of the most exploitable ones, with its field experiencing extensive development in recent years, mainly in photovoltaics [2]. Since the 1960s [3,4], natural sunlight has also been used to produce narrowband, collimated laser radiation in an efficient, simple, and reliable way, obviating the need for artificial pumping sources and their electrical power consumption and conditioning equipment. Solar laser is an emerging technology for both renewable energy and laser-based research and has been investigated as an instrument for materials processing [5] and optical communications [6], while showing great promise for space-based applications, such as wireless power transmission [7], deep-space optical data transmission and networking [8], laser propulsion [9], and asteroid deflection [10].

Even though solar laser emission is possible without any focusing optics [11], collectors and concentrators are normally employed to excite the active medium and obtain high efficiency. However, when using these components, the laser crystal is subjected to high power radiation, running the risk of experiencing significant thermal lens and thermal stress effects [12]. This has sparked researchers to look for ways to ameliorate the conditions for solar laser power production and reduce the probability of rod fracture, while being mindful of the laser efficiency. For example:

1. Nd:YAG proved to be a great rod material for highly intense solar pumping due to its availability, reasonably low cost, good thermomechanical properties [13], and spectroscopic properties of the dopant [14]. Sensitizers of the Nd<sup>3+</sup> ion emission, such as Cr<sup>3+</sup> and Ce<sup>3+</sup> ions, can also be added as co-dopants in the doped YAG host to increase the laser efficiency through the higher sunlight absorption and subsequent transfer of the excitation energy to the Nd<sup>3+</sup> ions [15,16].
2. Better heat dissipation and lessening of the thermal lens effect can be achieved through grooved rods, rather than the conventional rods with smooth sidewalls, since the area of contact between the laser medium and the cooling water is increased due to the shape of its sidewall, improving the laser efficiency and beam quality [17].
3. Multi-rod solar laser systems can facilitate an equal distribution of the total amount of concentrated radiation among the several rods [18–20]. This way, substantial improvement of the thermal performance can be achieved, in comparison with the single, thicker rod systems. The coordination of multiple laser beams, with each one being optimized to perform a part of the overall procedure, has also produced results that were unobtainable with a single beam in various laser-based applications [21–25].
4. Designing a solar laser system in side-pumping configuration can be constituted as a solution to provide alleviation of the thermal loading issue owed to the non-uniformity of the pump light distribution along the rod axis that is ubiquitous in the end-side-pumping approach, despite the latter being the configuration that has also led to record-breaking efficiencies [15,20,26–32]. Furthermore, the free access to both rod ends enables the optimization of more laser resonator parameters, permitting an efficient extraction of laser at low-order modes with improved beam quality [33–37]. This is of great significance for many laser-based applications in which the operation in TEM<sub>00</sub>-mode is desired due to the low divergence of the laser beam, allowing for a small, focused spot [38]. Damage in the resonator optics could also be prevented as a result of its smooth profile, avoiding the appearance of hot sites inside the laser medium [39].

The most significant results were achieved through heliostat-parabolic mirror systems. In 2017, 9.30 W continuous-wave (cw) TEM<sub>00</sub>-mode laser power was obtained by using a 1.18 m<sup>2</sup> effective collection area and a solar laser head composed of a fused silica aspheric lens and a conical pump cavity, in which a single Nd:YAG rod was mounted and end-side-pumped [30]. This corresponded to 7.88 W/m<sup>2</sup> collection and 0.79% solar-to-TEM<sub>00</sub>-mode-laser power conversion efficiencies. For multimode operation, the current record values were established in 2022 with the production of 16.50 W cw laser power from a 0.40 m<sup>2</sup> effective collection area and a similar laser head, this time with three Ce:Nd:YAG rods within the single pump cavity, with collection and conversion efficiencies reaching 41.25 W/m<sup>2</sup> and 4.64% [20], respectively. Nevertheless, using heliostat-parabolic mirror systems comes with a few drawbacks: namely, the need for complex and expensive installations to accommodate heavy components, and the blockage of sunlight redirected from the heliostat through the placement of the laser head and its supporting mechanics in front of the primary concentrator.

Albeit having inherent chromatic aberration properties, the collection and concentration of solar rays can be done through low-cost, lightweight, and easily available Fresnel lenses. In 2013, 2.30 W cw TEM<sub>00</sub>-mode laser power was obtained with a 1.00 m diameter Fresnel lens to side pump a single Nd:YAG rod, fixed inside a laser head comprised of a fused silica aspheric lens, a two-dimensional compound parabolic concentrator (CPC), and a V-shaped pump cavity [40]. The collection and conversion efficiencies were only 2.93 W/m<sup>2</sup> and 0.33%, respectively. In total, 26.93 W cw multimode laser power was produced in 2023 by end-side pumping a grooved Ce:Nd:YAG/YAG bonded crystal rod in a system that takes advantage of a 0.94 m diameter Fresnel lens and a laser head that consists of a conical cavity and a quartz tube, within which the rod was fixed [41]. This was equivalent to a 38.81 W/m<sup>2</sup> collection efficiency and a 3.88% conversion efficiency.

Due to all the reasons mentioned above, the lack of experimental works regarding TEM<sub>00</sub>-mode solar laser power production through Fresnel lenses (the most recent one being the aforementioned from 2013 [40], to the best of our knowledge) and the importance of studying the scalability of these systems, a seven-rod, side-pumping concept is presented here. Six Fresnel lenses with 10 m<sup>2</sup> total collection area, with the help of six folding mirrors, collected and concentrated sunlight towards a laser head composed of six aspheric lenses, six rectangular CPCs and a cylindrical pump cavity, within which seven grooved Nd:YAG rods were mounted and pumped. The design parameters were optimized using Zemax<sup>®</sup> (Kirkland, EA, USA) ray tracing in non-sequential mode and LASCAD<sup>™</sup> software (Munich, Germany). Efficient production of 153.29 W total TEM<sub>00</sub>-mode laser power could be achieved, corresponding to a 15.33 W/m<sup>2</sup> collection efficiency and a 1.61% solar-to-TEM<sub>00</sub>-mode-laser power conversion efficiency.

## 2. Description of the Seven-Rod TEM<sub>00</sub>-Mode Solar Laser Concept

The collection and first-stage concentration of solar rays were done by six Fresnel lenses, each with 0.73 m diameter and approximately 3.5 m focal length, totaling 10 m<sup>2</sup> of collection area. They were made of polymethylmethacrylate, which is a lightweight, clear, and stable polymer that has sunlight resistance, thermal stability up to at least 80 °C, and spectral transmissivity that matches the solar spectrum [42]. Six elliptical folding mirrors, with 1.5 m height, 1.0 m width, and 95% reflectivity, were tilted 45° to redirect the concentrated solar rays towards the laser head. Figure 1 depicts how the Fresnel lenses (FL<sub>1</sub>–FL<sub>6</sub>) and folding mirrors (M<sub>1</sub>–M<sub>6</sub>) were positioned in relation to it. The six pairs were divided into two groups: one was responsible for the concentration of solar rays towards the upper section of the laser head, while the other did the same for the lower section. In the upper-section group, the Fresnel lenses FL<sub>1</sub>, FL<sub>3</sub>, and FL<sub>5</sub> and folding mirrors M<sub>1</sub>, M<sub>3</sub>, and M<sub>5</sub> were positioned 1799.25 mm away from the optical axis of the laser head, with FL<sub>1</sub>, FL<sub>3</sub>, and FL<sub>5</sub> being 1637.50 mm above the middle of the laser head while M<sub>1</sub>, M<sub>3</sub>, and M<sub>5</sub> were only 6.75 mm above (=1630.75 mm below the corresponding Fresnel lens). In the lower-section group, the Fresnel lenses FL<sub>2</sub>, FL<sub>4</sub>, and FL<sub>6</sub> and folding mirrors M<sub>2</sub>, M<sub>4</sub>, and M<sub>6</sub> were positioned 1785.75 mm away from the optical axis of the laser head, with FL<sub>2</sub>, FL<sub>4</sub>, and FL<sub>6</sub> also being 1637.50 mm above the middle of the laser head, whereas M<sub>2</sub>, M<sub>4</sub>, and M<sub>6</sub> were 6.75 mm below (=1644.25 mm below the corresponding Fresnel lens).

Both the upper and lower sections of the laser head had three aspheric lenses and three rectangular CPCs that further concentrated the solar rays towards seven grooved Nd:YAG rods mounted inside a cylindrical pump cavity (Figure 2). The six aspheric lenses, each positioned on the same plane as the center of the corresponding folding mirror and 22 mm away from the optical axis of the laser head, had an input face of 110.0 mm diameter and –59 mm radius of curvature, and a plane output face of 25.4 mm diameter and 111 mm thickness. They were designed with fused silica material, which is transparent over the absorption spectrum of Nd:YAG and acts as a filter of undesired radiation, aside from having low thermal expansion coefficient and high resistance to scratching and thermal shock [43]. A rectangular CPC was placed below each aspheric lens, with its 21.4 × 16.2 mm<sup>2</sup> input face being 1.8 mm away from the lens's output face. The CPCs had an output face with 12.2 × 7.8 mm<sup>2</sup> area, 13.4 mm length, and inner mirrored walls with 95% reflectivity. The walls connecting the output edges of 12.2 mm with the input edges of 21.4 mm had an acceptance angle of 30°, whereas the walls perpendicular to those had a 26° acceptance angle.

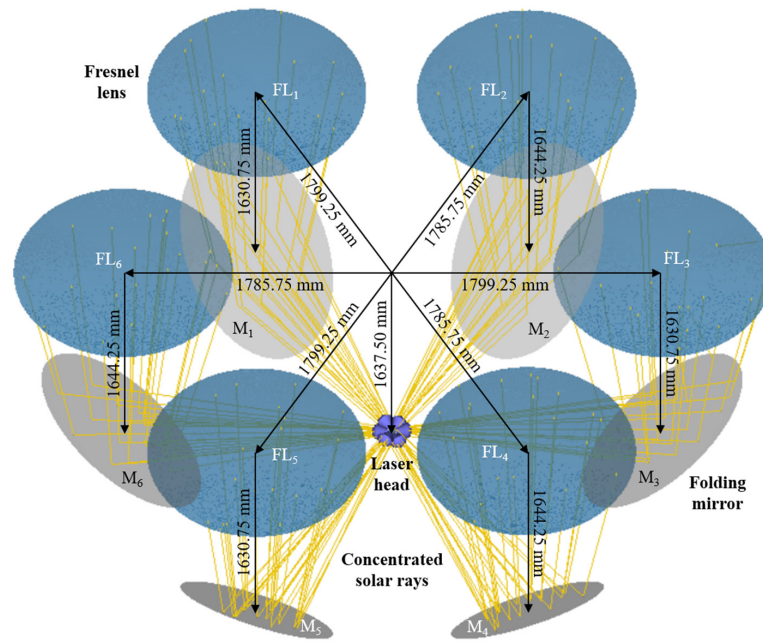


**Figure 1.** Collection and first-stage concentration system composed of six Fresnel lenses (FL<sub>1</sub>–FL<sub>6</sub>), with collection area totaling 10 m<sup>2</sup>, and six folding mirrors (M<sub>1</sub>–M<sub>6</sub>) that redirected the concentrated solar rays towards the laser head. FL<sub>1</sub>, FL<sub>3</sub>, and FL<sub>5</sub>, and M<sub>1</sub>, M<sub>3</sub>, and M<sub>5</sub> were responsible for the concentration of solar rays towards the upper section of the laser head; FL<sub>2</sub>, FL<sub>4</sub>, and FL<sub>6</sub>, and M<sub>2</sub>, M<sub>4</sub>, and M<sub>6</sub> had the same role for the lower section.

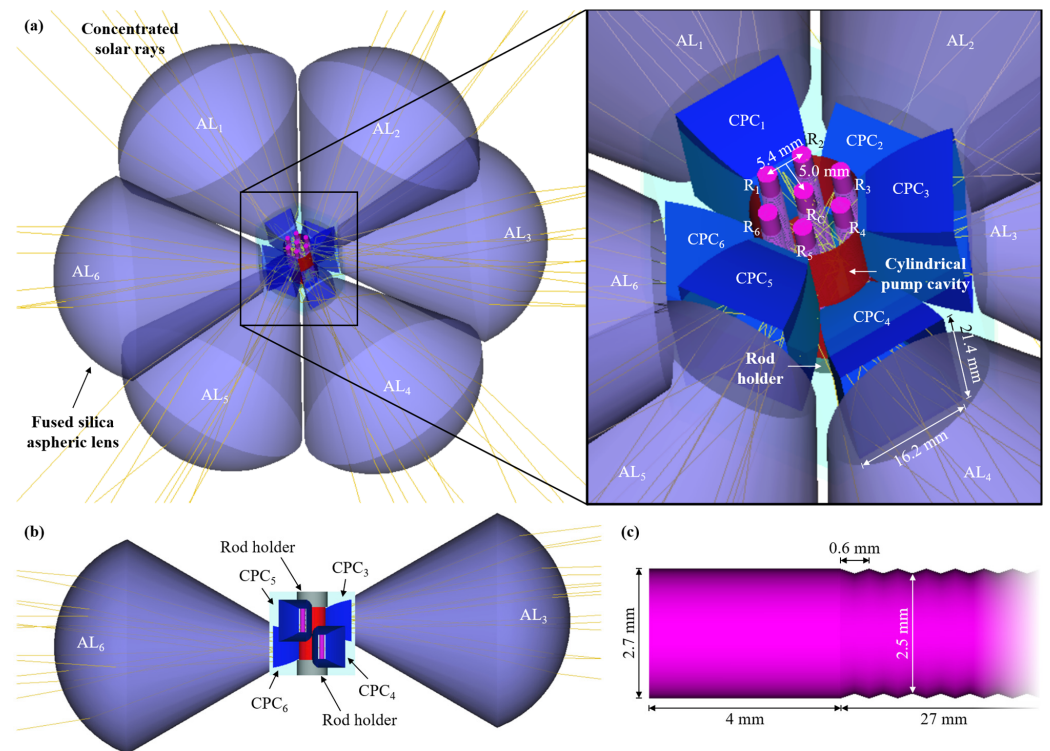


**Figure 2.** (a) Three-dimensional and (b) side views of the solar laser head. The rod holder from the upper section in (a) and fused silica aspheric lenses AL<sub>1</sub>, AL<sub>2</sub>, AL<sub>4</sub>, and AL<sub>5</sub> in (b) were hidden for better visualization of the pump cavity. AL<sub>1</sub>, AL<sub>3</sub>, and AL<sub>5</sub>, and CPC<sub>1</sub>, CPC<sub>3</sub>, and CPC<sub>5</sub> were responsible for the further concentration of solar rays in the upper section of the pump cavity; AL<sub>2</sub>, AL<sub>4</sub>, and AL<sub>6</sub>, and CPC<sub>2</sub>, CPC<sub>4</sub>, and CPC<sub>6</sub> had the same role in the lower section. (c) End of one of the grooved rods designed in Zemax<sup>®</sup>.

The cylindrical pump cavity was a mirrored pipe with 15.7 mm diameter, 27.0 mm length, and 95% reflectivity. It had six  $13.5 \times 7.8 \text{ mm}^2$  area openings for the entrance of solar rays, with the 7.8 mm edges being connected with those of the CPCs. Each end of the cavity was closed with a rod holder of the same diameter and reflectivity for the mechanical fixation of 4 mm of the corresponding ends of the seven 2.7 mm diameter, 35 mm length grooved Nd:YAG rods (Figure 2b). The rods, apart from the 4 mm at each end reserved for the holder, had grooves along their length (Figure 2c) akin to those on the active media utilized in previous experimental works performed by our research group [36,44]: with 0.6 mm pitch and 0.1 mm depth. Additionally, the end faces of each rod presented a coating that is antireflective (AR) to the 1064 nm laser emission wavelength. As shown in Figure 2, one rod was positioned at the center of the pump cavity ( $R_C$ ), while the other six were grouped into three pairs ( $R_1$  and  $R_2$ ,  $R_3$  and  $R_4$ , and  $R_5$  and  $R_6$ ). Each pair was placed 5 mm away from the center of the cavity, while the optical axes of the grooved rods were 5.4 mm away from each other.

The plane output face of the aspheric lenses, the CPCs, the cylindrical pump cavity and the seven grooved rods were in direct contact with cooling water, entering from the CPCs of the upper section ( $CPC_1$ ,  $CPC_3$ , and  $CPC_5$ ) and exiting from the ones at the lower section of the pump cavity ( $CPC_2$ ,  $CPC_4$ , and  $CPC_6$ ) to help diminish the heat generation within the rods and the optical components.

Each of the seven laser resonators was comprised of two opposing mirrors aligned with the optical axis of the grooved rod, both with different coatings: highly reflective (HR) and partially reflective (PR) to the 1064 nm laser emission wavelength, through which the solar laser was emitted (Figure 3).

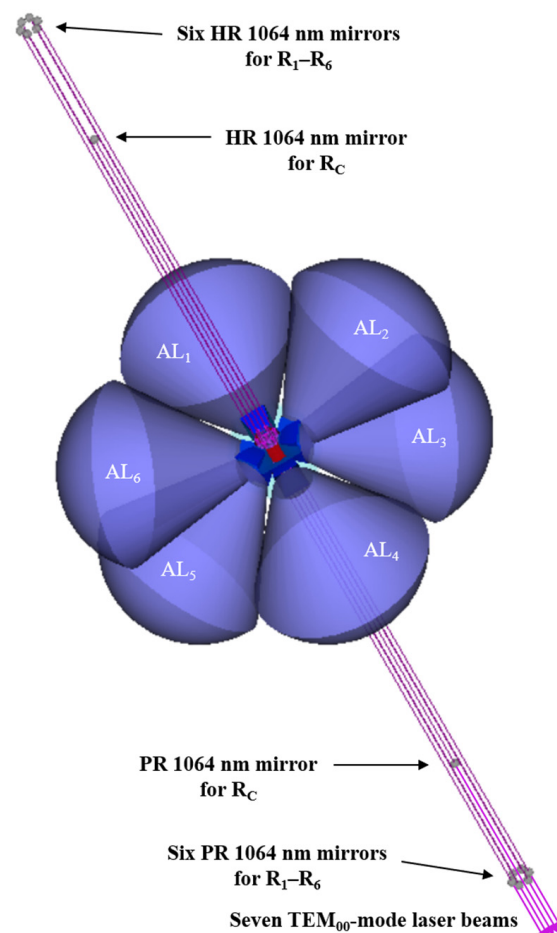


**Figure 3.** Three-dimensional view of the laser head with the laser resonators for rods  $R_C$  and  $R_1$ - $R_6$ .

### 3. Numerical Modeling

#### 3.1. Modeling of the Design Parameters of the TEM<sub>00</sub>-Mode Solar Laser System through Zemax<sup>®</sup>

Preparations to the Zemax<sup>®</sup> file prior to the design parameter optimization were done. A 950 W/m<sup>2</sup> terrestrial solar irradiance and the 16% overlap that the Nd:YAG absorption spectrum has with the solar spectrum [45] were considered when calculating the effective pump power for each of the six light sources. After consultation of the direct standard solar spectrum for one-and-a-half air mass [46], 22 spectral irradiance values at the peak absorption wavelength for the 1.0 at.% Nd:YAG material, as well as the absorption coefficient for each of those wavelengths [47], were used as reference data for the light sources and in the glass catalog data for Nd:YAG, respectively. Both the absorption spectra and the wavelength-dependent refractive indices of fused silica and water [32] were also added to the glass catalog data to account for the absorption losses that occur in those media.

The numerical information from each rod was obtained using a detector volume. The absorbed pump power in each rod was calculated by summing up the power in each of the 87,500 voxels that the detector volume was comprised of. This number of voxels, along with  $6 \times 10^6$  analysis rays, enabled the acquisition of accurate results and good image resolution from each detector. The absorbed pump flux distribution in five transversal cross-sections of the seven grooved Nd:YAG rods and in the longitudinal cross-section of rods R<sub>C</sub> and R<sub>1</sub> is presented in Figure 4. Longitudinal profiles for rods R<sub>2</sub>–R<sub>6</sub> were not included, as they are similar to that of rod R<sub>1</sub>. The maximum pump flux is represented in red, whereas the blue color identifies the areas of the rods where there was little or no absorption.

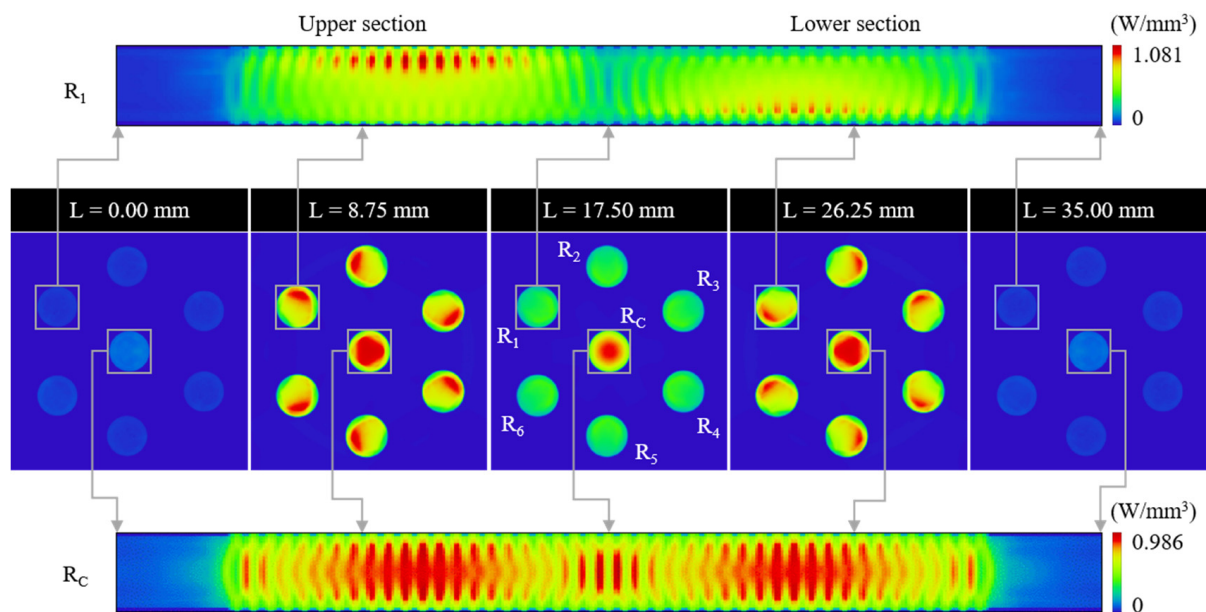


**Figure 4.** Absorbed pump flux distribution in five transversal cross-sections of the seven 2.7 mm diameter, 35 mm length, grooved Nd:YAG rods, as well as in the longitudinal cross-section of the rods R<sub>C</sub> and R<sub>1</sub>. L represents the position where each transversal cross-section profile was obtained.

Each time the ray tracing finished performing, the absorbed pump flux data were exported from Zemax<sup>®</sup> to be used in the LASCAD<sup>™</sup> software afterwards. The quantification of the thermal effects applied to the active media and the highest solar laser output power provided by the optimal resonator beam parameters in each case determined what modifications were to be made to the design parameters to possibly lead to further enhancements in TEM<sub>00</sub>-mode laser power and beam quality.

### 3.2. Modeling of the Laser Resonator Parameters through LASCAD™ for TEM<sub>00</sub>-Mode Laser Beam Extraction

In LASCAD™, the data analysis was done while considering a temperature-dependent stimulated emission cross-section given by:

$$\sigma(T) = 2.8 \times 10^{-19} - 3.9 \times 10^{-22}(T - 300), \tag{1}$$

where  $2.8 \times 10^{-19} \text{ cm}^2$  is the stimulated emission cross-section at 300 K [39],  $-3.9 \times 10^{-22} \text{ cm}^2/\text{K}$  is the slope of the linear relationship between stimulated emission cross-section and temperature for the 1.0 at.% Nd:YAG medium [48], and  $T$  the maximum temperature that the rod achieved. The 230  $\mu\text{s}$  fluorescence lifetime [39], the  $0.002 \text{ cm}^{-1}$  absorption and scattering loss for the 1.0 at.% Nd:YAG medium, and the 660 nm mean-absorbed and intensity weighted solar pump wavelength [13] were also considered.

Each laser resonator was comprised of the two mirrors with the HR and PR 1064 nm coatings (reflectivity of 99.98% and 90–99%, respectively), whose optical axes were aligned with that of the rod. The resonator length plays a crucial role in the extraction of the TEM<sub>00</sub>-mode laser beam. In short resonators, the TEM<sub>00</sub>-mode poorly matches the active region, and the laser oscillates in multiple modes, leading to high beam quality factors ( $M_x^2$ ,  $M_y^2$ ). By increasing its length, the TEM<sub>00</sub>-mode beam size within the rod also increases, along with the diffraction losses at the rod edges, leading to the elimination of higher order modes. Long resonators were chosen so that only the TEM<sub>00</sub>-mode could oscillate, improving the beam quality [39]. To facilitate the oscillation of the TEM<sub>00</sub>-mode, small diameter laser rods were used due to their behavior as apertures. The separation length and radius of curvature (RoC) of the resonator mirrors were also optimized.

Figures 5 and 6 show the laser resonator design for the extraction of a TEM<sub>00</sub>-mode laser beam from the rods R<sub>C</sub> and R<sub>1</sub>, respectively. It is worth pointing out that the laser resonators for rods R<sub>2</sub>–R<sub>6</sub> are similar to that of R<sub>1</sub>. To extract the most efficient TEM<sub>00</sub>-mode laser beam from rod R<sub>C</sub>, HR and PR 1064 nm mirrors with an 8000 mm RoC and a 305.6 mm separation length on each side were used; this enabled the emission of a 27.11 W laser beam with good quality factors of  $M_x^2 = 2.25$ ,  $M_y^2 = 1.00$ . On the other hand, the laser resonators for rods R<sub>1</sub>–R<sub>6</sub> were longer, with 850 mm RoC mirrors and 423.8 mm separation lengths, resulting in six 21.03 W laser beams with even better quality factors ( $M_x^2 = 1.09$ ,  $M_y^2 = 1.00$ ) than those from rod R<sub>C</sub>.

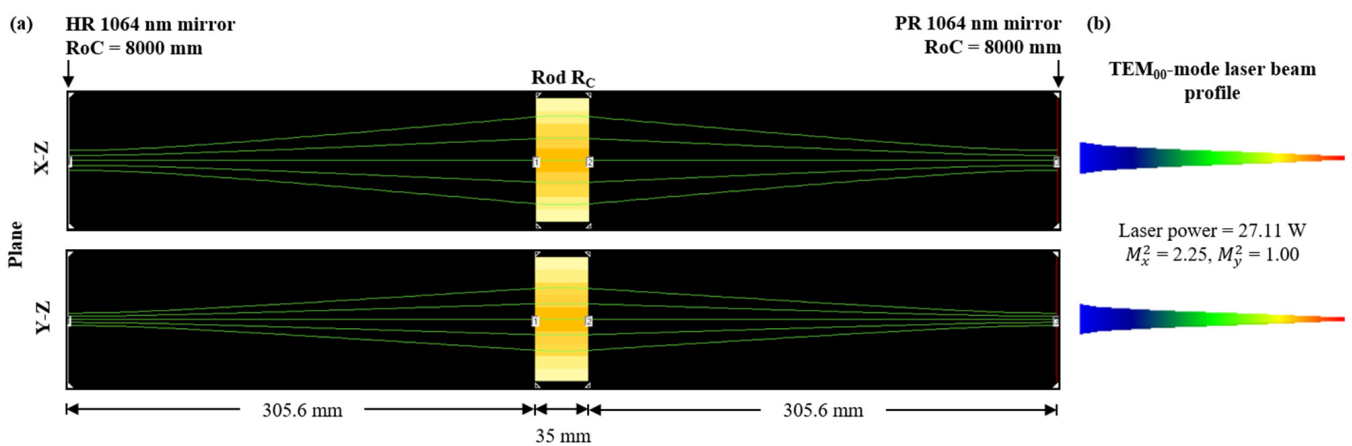
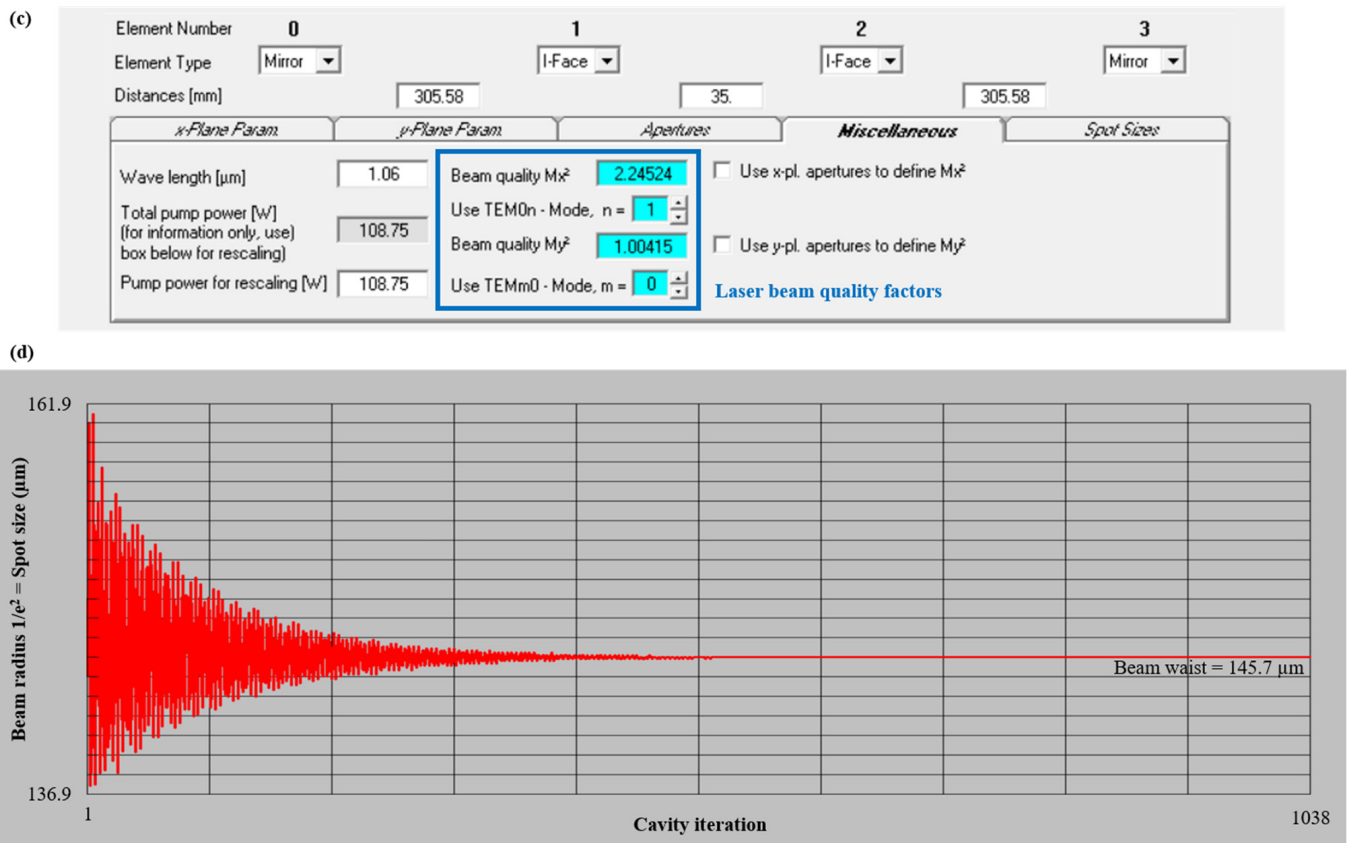
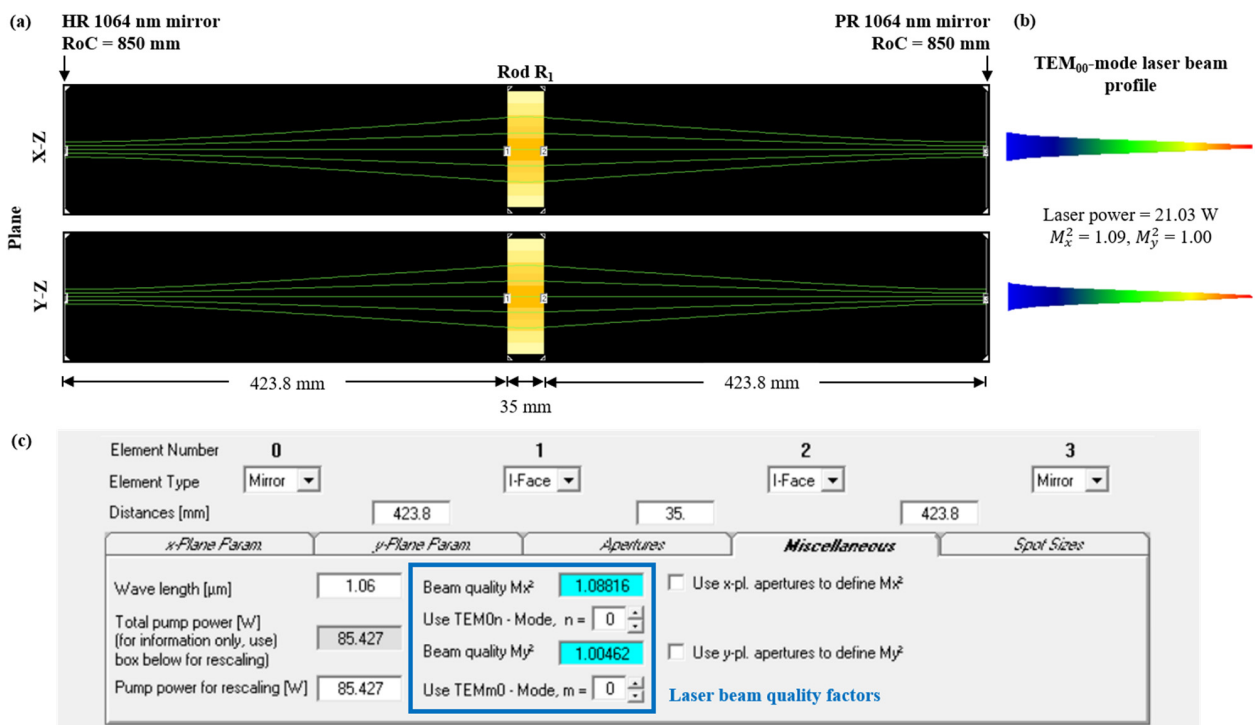


Figure 5. Cont.



**Figure 5.** (a) Laser resonator design in LASCAD™ for the extraction of a TEM<sub>00</sub>-mode laser beam from rod R<sub>C</sub>, with (b) the respective beam profile. (c) LASCAD™ window in which the laser beam quality factors  $M_x^2$ ,  $M_y^2$  are presented. (d) Laser beam waist radius obtained at the PR 1064 nm output mirror, through the LASCAD™ beam propagation method.



**Figure 6.** Cont.

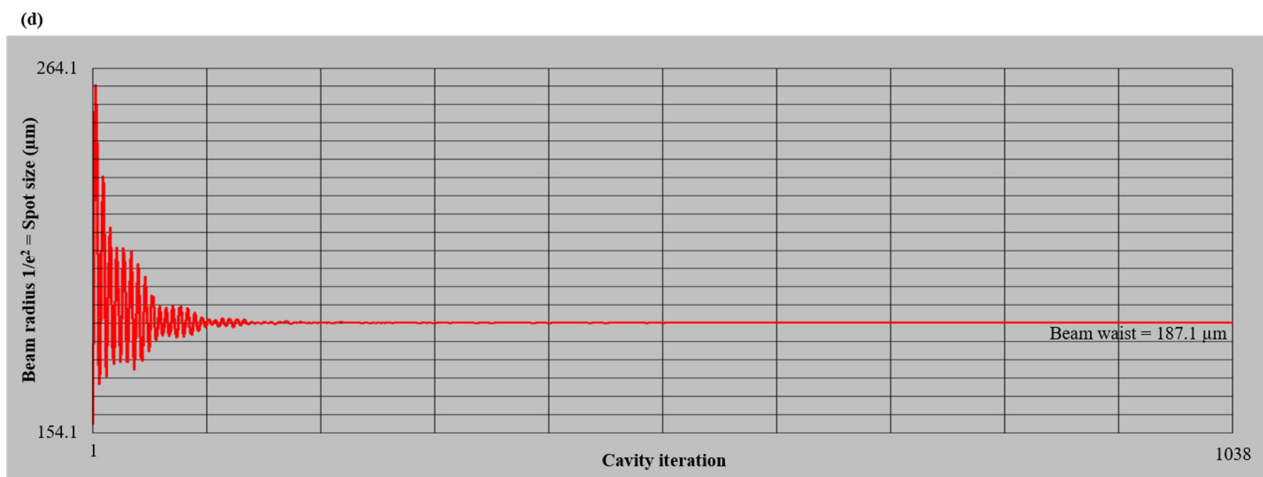


**Figure 6.** (a) Laser resonator design in LASCAD™ for the extraction of a TEM<sub>00</sub>-mode laser beam from rod R<sub>1</sub>, with (b) the respective beam profile. (c) LASCAD™ window in which the laser beam quality factors  $M_x^2$ ,  $M_y^2$  are presented. (d) Laser beam waist radius obtained at the PR 1064 nm output mirror, through the LASCAD™ beam propagation method.

#### 4. Numerical Analysis of the Seven-Rod TEM<sub>00</sub>-Mode Solar Laser System

##### 4.1. Laser Power Analysis

The optimization process was firstly conducted for a scheme in which conventional rods were used. After finding the parameters with which the maximum TEM<sub>00</sub>-mode laser power could be achieved, the rods were substituted by ones with grooved sidewalls. Figure 7 presents the total TEM<sub>00</sub>-mode laser power as a function of the rod length using rods with the optimal diameter of 2.7 mm for both the conventional and the grooved rod schemes. In the conventional rod scheme, the maximum total laser power was 139.89 W (=25.53 + 6 × 19.06), attained with 2.7 mm diameter and 35 mm length rods, corresponding to collection and solar-to-TEM<sub>00</sub>-mode-laser power conversion efficiencies of 13.99 W/m<sup>2</sup> and 1.47%, respectively. However, the adoption of grooved rods of the same dimensions increased the laser power that each of the seven rods would produce, totaling 153.29 W (=27.11 + 6 × 21.03). Collection efficiency, in this case, was 15.33 W/m<sup>2</sup>, whereas the conversion efficiency reached 1.61%.

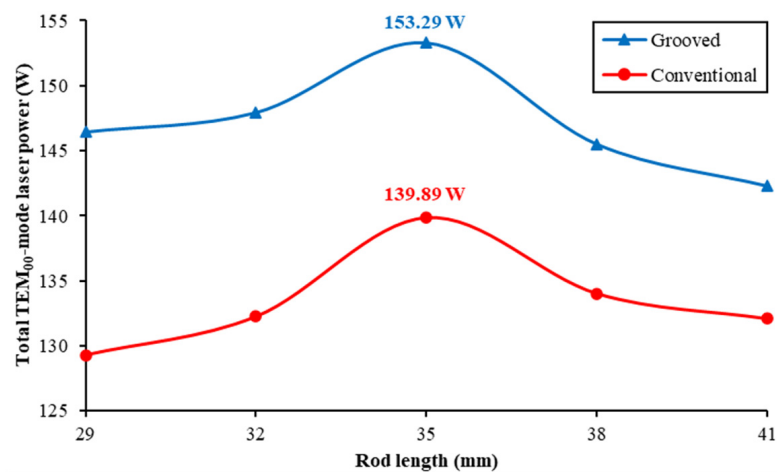


**Figure 7.** Total TEM<sub>00</sub>-mode laser power as a function of rod length, for the conventional and the grooved Nd:YAG rod schemes while using rods with 2.7 mm diameter.

#### 4.2. Thermal Analysis

The thermal-induced effects—heat load, temperature, and stress intensity—on rods  $R_C$  and  $R_1$  from the conventional and the grooved rod schemes were analyzed through LASCAD™ and are presented in Figure 8.

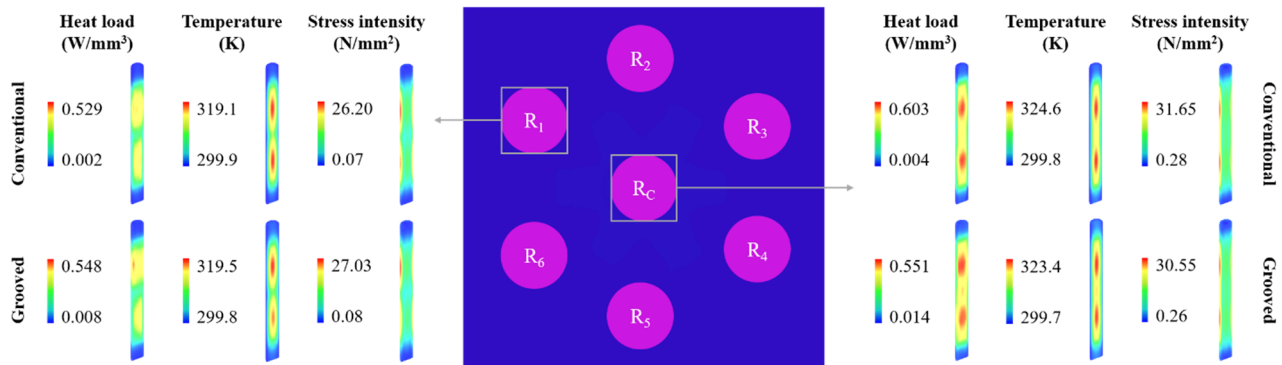


**Figure 8.** Heat load, temperature, and stress intensity for rods  $R_C$  and  $R_1$  from both the conventional and the grooved Nd:YAG rod schemes.

Due to opting for the side-pumping configuration and how small their diameter was, the grooved rods ended up not playing a very relevant role in heat dissipation. For rod  $R_C$ , the grooved sidewall provided a modicum of alleviation when compared to the conventional one, registering decreases in the maximum heat load, temperature, and stress intensity of only 8.62%, 0.37%, and 3.48%, respectively. For rod  $R_1$ , the opposite scenario transpired, with the difference between values being even lower: heat load was 3.59%, temperature 0.13%, and stress intensity 3.17% higher with the grooved rod. Nevertheless, in both case studies, the stress intensity was always substantially lower than the stress fracture limit of 200 N/mm<sup>2</sup> for the Nd:YAG material [49], reflecting a potential good performance of the rods under highly intense solar pumping.

#### 5. Discussion

In the proposed seven-rod TEM<sub>00</sub>-mode solar laser scheme, opting for rods with grooved sidewalls instead of the conventional ones proved to be an added value to increase its efficiency, despite not being sufficiently pertinent in providing better heat dissipation. This constituted improvements in comparison to other numerical works in which Fresnel lenses were used as the collectors and primary concentrators. Table 1 summarizes the results of the present work and those from two other numerical studies of highly efficient TEM<sub>00</sub>-mode laser power production schemes by Liang et al. [50,51]:

1. A single-rod scheme, in which four Fresnel lenses with 4 m<sup>2</sup> total collection area, with the help of folding mirrors, collected and concentrated the solar rays towards a laser head composed of four fused silica aspheric lenses with long rectangular light guides for solar flux homogenization, four hollow rectangular CPCs, and four V-shaped pump cavities, where a 3 mm diameter and 76 mm length conventional Nd:YAG rod was mounted [50].
2. A seven-rod scheme, where a single 4 m<sup>2</sup> collection area Fresnel lens collected and concentrated the solar rays, being then received by a laser head comprised of a fused silica aspheric lens, a conical pump cavity, and seven 2.5 mm diameter and 15 mm length conventional Nd:YAG rods [51].

The proposed seven-grooved-rod scheme is 1.04 times more efficient than the single-rod scheme by Liang et al. [50], as well as being able to produce six laser beams of better quality. Moreover, thermal lens and thermal stress effects can be more pronounced in the single-rod scheme than in the one proposed here. On the other hand, the seven-rod scheme by Liang et al. produced seven laser beams of overall better quality [51]; however, not only

is the proposed scheme 1.12 times more efficient, but a 4 m<sup>2</sup> collection area Fresnel lens is also not easily available on the market, which is a major deterrent for experimental testing, as opposed to six smaller Fresnel lenses with a 10 m<sup>2</sup> total collection area.

**Table 1.** Comparison between the results of the present work and those from [50,51].

Parameter	Liang et al. (2014) [50]	Liang et al. (2021) [51]	Present Work
Type of rod	Conventional	Conventional	Grooved
Number of rods	1	7	7
Configuration	Side-pumping	End-side-pumping	Side-pumping
Number of Fresnel lenses	4	1	6
Collection area (m <sup>2</sup> )	4	4	10
Solar irradiance (W/m <sup>2</sup> )	950	950	950
Total TEM <sub>00</sub> -mode laser power (W)	59.10	54.64 (=7.85 + 6 × 7.80)	153.29 (=27.11 + 6 × 21.03)
Collection efficiency (W/m <sup>2</sup> )	14.78	13.66	15.33
Conversion efficiency (%)	1.56	1.44	1.61
$M_x^2, M_y^2$	1.08, 1.43	1 × (1.36, 1.00) 6 × (1.00, 1.04)	1 × (2.25, 1.00) 6 × (1.09, 1.00)

Due to the disposition of the rods and the side-pumping configuration, a laser beam merging could be performed in the proposed scheme to combine the six individual TEM<sub>00</sub>-mode laser beams from the external rods, with the help of folding mirrors [52], enabling the extraction of a single laser beam with higher power and better quality. However, this laser beam merging technique cannot be employed in the seven-rod scheme by Liang et al. [51], since the rod tilting and the end-side-pumping configuration do not make it possible for the folding mirrors to be mechanically fixed.

### 6. Conclusions

A seven-rod solar laser concept was proposed here to improve the efficiency in TEM<sub>00</sub>-mode laser power production, employing six Fresnel lenses with 10 m<sup>2</sup> total collection area for collection and concentration of sunlight. Six folding mirrors redirected the solar rays towards the laser head comprised of six aspheric lenses, six rectangular CPCs, and a cylindrical cavity, in which seven Nd:YAG rods were mounted and side-pumped. With 2.7 mm diameter and 35 mm length conventional rods, 139.89 W total TEM<sub>00</sub>-mode laser power was numerically achieved, which is equivalent to a 13.99 W/m<sup>2</sup> collection efficiency and a 1.47% solar-to-TEM<sub>00</sub>-mode-laser power conversion efficiency. By adopting grooved rods of the same dimensions, the total laser power was increased to 153.29 W, corresponding to 15.33 W/m<sup>2</sup> collection and 1.61% conversion efficiencies. Regarding TEM<sub>00</sub>-mode laser power production through the usage of Fresnel lenses, the proposed seven-grooved-rod scheme is 1.04 times more efficient than the one that held the previous numerical record, in which a single conventional rod was side-pumped [50]. It is also 1.12 times more efficient than another seven-conventional-rod concept, designed in the end-side-pumping configuration [51]. Furthermore, the side-pumping configuration paired with the good thermal performance may ensure the seven-grooved-rod system has better scalability than these previously proposed schemes, as well as opening the possibility for the application of a laser beam merging technique.

The implementation of Cr:Nd:YAG [15] or Ce:Nd:YAG [16] rods could lead to further improvements in efficiency, depending on how well the absorption spectra of these materials match with the solar spectrum. The use of easily available Fresnel lenses and the possibility of producing multiple TEM<sub>00</sub>-mode laser beams of high efficiency reinforce the importance that solar lasers could have in many laser-based applications.

**Author Contributions:** Conceptualization, D.L., H.C. and J.A.; methodology, H.C., D.L., J.A. and C.R.V.; software, H.C., D.L., J.A. and D.G.; validation, H.C., D.L. and J.A.; formal analysis, H.C., D.L., J.A., M.C. and B.D.T.; investigation, H.C., D.L. and J.A.; resources, D.L. and J.A.; data curation, H.C., D.L. and J.A.; writing—original draft preparation, H.C.; writing—review and editing, H.C., D.L., J.A., M.C., D.G., B.D.T. and C.R.V.; visualization, H.C.; supervision, D.L. and J.A.; project administration, D.L.; funding acquisition, D.L. All authors have read and agreed to the published version of the manuscript.

**Funding:** This research was funded by Fundação para a Ciência e a Tecnologia—Ministério da Ciência, Tecnologia e Ensino Superior (FCT—MCTES), grant UIDB/00068/2020.

**Institutional Review Board Statement:** Not applicable.

**Informed Consent Statement:** Not applicable.

**Data Availability Statement:** Not applicable.

**Acknowledgments:** The FCT-MCTES fellowship grants 2021.06172.BD, CEECIND/03081/2017, SFRH/BD/145322/2019, PD/BD/142827/2018, and SFRH/BPD/125116/2016 of Hugo Costa, Joana Almeida, Miguel Catela, Dário Garcia, and Cláudia R. Vistas, respectively, are acknowledged.

**Conflicts of Interest:** The authors declare no conflict of interest. The funders had no role in the design of the study; in the collection, analyses, or interpretation of data; in the writing of the manuscript; or in the decision to publish the results.

## References

1. IEA Renewable Power's Growth Is Being Turbocharged as Countries Seek to Strengthen Energy Security. Available online: <https://www.iea.org/news/renewable-power-s-growth-is-being-turbocharged-as-countries-seek-to-strengthen-energy-security> (accessed on 2 February 2023).
2. McKinsey Renewable-Energy Development in a Net-Zero World. Available online: <https://www.mckinsey.com/industries/electric-power-and-natural-gas/our-insights/renewable-energy-development-in-a-net-zero-world> (accessed on 2 February 2023).
3. Kiss, Z.J.; Lewis, H.R.; Duncan, R.C., Jr. Sun Pumped Continuous Optical Maser. *Appl. Phys. Lett.* **1963**, *2*, 93–94. [CrossRef]
4. Young, C.G. A Sun-Pumped CW One-Watt Laser. *Appl. Opt.* **1966**, *5*, 993. [CrossRef]
5. Yabe, T.; Bagheri, B.; Ohkubo, T.; Uchida, S.; Yoshida, K.; Funatsu, T.; Oishi, T.; Daito, K.; Ishioka, M.; Yasunaga, N.; et al. 100 W-Class Solar Pumped Laser for Sustainable Magnesium-Hydrogen Energy Cycle. *J. Appl. Phys.* **2008**, *104*, 083104. [CrossRef]
6. Guan, Z.; Zhao, C.M.; Yang, S.H.; Wang, Y.; Ke, J.Y.; Zhang, H.Y. Demonstration of a Free-Space Optical Communication System Using a Solar-Pumped Laser as Signal Transmitter. *Laser Phys. Lett.* **2017**, *14*, 055804. [CrossRef]
7. Lando, M.; Kagan, J.A.; Shimony, Y.; Kalisky, Y.Y.; Noter, Y.; Yogev, A.; Rotman, S.R.; Rosenwaks, S. Solar-Pumped Solid State Laser Program. In Proceedings of the 10th Meeting on Optical Engineering in Israel, Jerusalem, Israel, 22 September 1997; Shladov, I., Rotman, S.R., Eds.; SPIE: Bellingham, WA, USA; Volume 3110, p. 196.
8. Hemmati, H.; Biswas, A.; Djordjevic, I.B. Deep-Space Optical Communications: Future Perspectives and Applications. In *Proceedings of the IEEE*; IEEE: Piscataway, NJ, USA, 2011; Volume 99, pp. 2020–2039.
9. Rather, J.D.G.; Gerry, E.T.; Zeiders, G.W. Investigation of Possibilities for Solar Powered High Energy Lasers in Space. *NASA Tech. Rep. Serv.* **1977**. Available online: <https://ntrs.nasa.gov/citations/19820010707> (accessed on 2 February 2023).
10. Vasile, M.; Maddock, C.A. Design of a Formation of Solar Pumped Lasers for Asteroid Deflection. *Adv. Space Res.* **2012**, *50*, 891–905. [CrossRef]
11. Masuda, T.; Iyoda, M.; Yasumatsu, Y.; Dottermusch, S.; Howard, I.A.; Richards, B.S.; Bisson, J.-F.; Endo, M. A Fully Planar Solar Pumped Laser Based on a Luminescent Solar Collector. *Commun. Phys.* **2020**, *3*, 60. [CrossRef]
12. Hwang, I.H.; Lee, J.H. Efficiency and Threshold Pump Intensity of CW Solar-Pumped Solid-State Lasers. *IEEE J. Quantum Electron.* **1991**, *27*, 2129–2134. [CrossRef]
13. Weksler, M.; Shwartz, J. Solar-Pumped Solid-State Lasers. *IEEE J. Quantum Electron.* **1988**, *24*, 1222–1228. [CrossRef]
14. Lupei, V.; Lupei, A.; Gheorghie, C.; Ikesue, A. Emission Sensitization Processes Involving Nd<sup>3+</sup> in YAG. *J. Lumin.* **2016**, *170*, 594–601. [CrossRef]
15. Liang, D.; Vistas, C.R.; Tibúrcio, B.D.; Almeida, J. Solar-Pumped Cr:Nd:YAG Ceramic Laser with 6.7% Slope Efficiency. *Sol. Energy Mater. Sol. Cells* **2018**, *185*, 75–79. [CrossRef]
16. Vistas, C.R.; Liang, D.; Almeida, J.; Tibúrcio, B.D.; Garcia, D.; Catela, M.; Costa, H.; Guillot, E. Ce:Nd:YAG Side-Pumped Solar Laser. *J. Photonics Energy* **2021**, *11*, 018001. [CrossRef]
17. Guan, Z.; Zhao, C.; Yang, S.; Wang, Y.; Ke, J.; Gao, F.; Zhang, H. Low Threshold and High Efficiency Solar-Pumped Laser with Fresnel Lens and a Grooved Nd:YAG Rod. In Proceedings of the High-Power Lasers and Applications VIII, Beijing, China, 9 November 2016; Li, R., Singh, U.N., Walter, R.F., Eds.; SPIE: Bellingham, WA, USA; Volume 10016, p. 1001609.
18. Liang, D.; Almeida, J.; Garcia, D.; Tibúrcio, B.D.; Guillot, E.; Vistas, C.R. Simultaneous Solar Laser Emissions from Three Nd:YAG Rods within a Single Pump Cavity. *Sol. Energy* **2020**, *199*, 192–197. [CrossRef]

19. Tibúrcio, B.D.; Liang, D.; Almeida, J.; Garcia, D.; Catela, M.; Costa, H.; Vistas, C.R. Tracking Error Compensation Capacity Measurement of a Dual-Rod Side-Pumping Solar Laser. *Renew. Energy* **2022**, *195*, 1253–1261. [[CrossRef](#)]
20. Liang, D.; Vistas, C.R.; Garcia, D.; Tibúrcio, B.D.; Catela, M.; Costa, H.; Guillot, E.; Almeida, J. Most Efficient Simultaneous Solar Laser Emissions from Three Ce:Nd:YAG Rods within a Single Pump Cavity. *Sol. Energy Mater. Sol. Cells* **2022**, *246*, 111921. [[CrossRef](#)]
21. Olsen, F.O.; Hansen, K.S.; Nielsen, J.S. Multibeam Fiber Laser Cutting. *J. Laser Appl.* **2009**, *21*, 133–138. [[CrossRef](#)]
22. Eifel, S.; Holtkamp, J. Multi-Beam Technology Boosts Cost Efficiency. Available online: <https://www.laserfocusworld.com/industrial-laser-solutions/article/14216434/multibeam-technology-boosts-cost-efficiency> (accessed on 10 February 2023).
23. Strite, T.; Gusenko, A.; Grupp, M.; Hoult, T. Multiple Laser Beam Material Processing. *Biul. Inst. Spaw.* **2016**, *60*, 30–33. [[CrossRef](#)]
24. Gillner, A.; Finger, J.; Gretzki, P.; Niessen, M.; Bartels, T.; Reininghaus, M. High Power Laser Processing with Ultrafast and Multi-Parallel Beams. *J. Laser Micro Nanoeng.* **2019**, *14*, 129–137. [[CrossRef](#)]
25. Thibault, F. Multibeam Laser Marking: The Individual Traceability Enabler. Available online: <https://www.laserfocusworld.com/laser-processing/article/14270572/laser-marking-the-individual-traceability-enabler> (accessed on 10 February 2023).
26. Yabe, T.; Ohkubo, T.; Uchida, S.; Yoshida, K.; Nakatsuka, M.; Funatsu, T.; Mabuti, A.; Oyama, A.; Nakagawa, K.; Oishi, T.; et al. High-Efficiency and Economical Solar-Energy-Pumped Laser with Fresnel Lens and Chromium Codoped Laser Medium. *Appl. Phys. Lett.* **2007**, *90*, 261120. [[CrossRef](#)]
27. Liang, D.; Almeida, J. Highly Efficient Solar-Pumped Nd:YAG Laser. *Opt. Express* **2011**, *19*, 26399. [[CrossRef](#)]
28. Dinh, T.H.; Ohkubo, T.; Yabe, T.; Kuboyama, H. 120 Watt Continuous Wave Solar-Pumped Laser with a Liquid Light-Guide Lens and an Nd:YAG Rod. *Opt. Lett.* **2012**, *37*, 2670. [[CrossRef](#)]
29. Xu, P.; Yang, S.; Zhao, C.; Guan, Z.; Wang, H.; Zhang, Y.; Zhang, H.; He, T. High-Efficiency Solar-Pumped Laser with a Grooved Nd:YAG Rod. *Appl. Opt.* **2014**, *53*, 3941. [[CrossRef](#)] [[PubMed](#)]
30. Liang, D.; Almeida, J.; Vistas, C.R.; Guillot, E. Solar-Pumped Nd:YAG Laser with 31.5 W/m<sup>2</sup> Multimode and 7.9 W/m<sup>2</sup> TEM<sub>00</sub>-Mode Collection Efficiencies. *Sol. Energy Mater. Sol. Cells* **2017**, *159*, 435–439. [[CrossRef](#)]
31. Guan, Z.; Zhao, C.; Li, J.; He, D.; Zhang, H. 32.1 W/m<sup>2</sup> Continuous Wave Solar-Pumped Laser with a Bonding Nd:YAG/YAG Rod and a Fresnel Lens. *Opt. Laser Technol.* **2018**, *107*, 158–161. [[CrossRef](#)]
32. Garcia, D.; Liang, D.; Vistas, C.R.; Costa, H.; Catela, M.; Tibúrcio, B.D.; Almeida, J. Ce:Nd:YAG Solar Laser with 4.5% Solar-to-Laser Conversion Efficiency. *Energies* **2022**, *15*, 5292. [[CrossRef](#)]
33. Lando, M.; Kagan, J.; Linyekin, B.; Dobrusin, V. A Solar-Pumped Nd:YAG Laser in the High Collection Efficiency Regime. *Opt. Commun.* **2003**, *222*, 371–381. [[CrossRef](#)]
34. Liang, D.; Almeida, J.; Vistas, C.R.; Guillot, E. Solar-Pumped TEM<sub>00</sub> Mode Nd:YAG Laser by a Heliostat-Parabolic Mirror System. *Sol. Energy Mater. Sol. Cells* **2015**, *134*, 305–308. [[CrossRef](#)]
35. Almeida, J.; Liang, D.; Vistas, C.R.; Bouadjemine, R.; Guillot, E. 5.5 W Continuous-Wave TEM<sub>00</sub>-Mode Nd:YAG Solar Laser by a Light-Guide/2V-Shaped Pump Cavity. *Appl. Phys. B* **2015**, *121*, 473–482. [[CrossRef](#)]
36. Vistas, C.R.; Liang, D.; Almeida, J.; Guillot, E. TEM<sub>00</sub> Mode Nd:YAG Solar Laser by Side-Pumping a Grooved Rod. *Opt. Commun.* **2016**, *366*, 50–56. [[CrossRef](#)]
37. Liang, D.; Almeida, J.; Vistas, C.R.; Oliveira, M.; Gonçalves, F.; Guillot, E. High-Efficiency Solar-Pumped TEM<sub>00</sub>-Mode Nd:YAG Laser. *Sol. Energy Mater. Sol. Cells* **2016**, *145*, 397–402. [[CrossRef](#)]
38. Duocastella, M.; Arnold, C.B. Bessel and Annular Beams for Materials Processing. *Laser Photonics Rev.* **2012**, *6*, 607–621. [[CrossRef](#)]
39. Koehner, W. *Solid-State Laser Engineering*, 5th ed.; Springer Series in Optical Sciences; Springer: Berlin/Heidelberg, Germany, 1999; Volume 1, ISBN 978-3-662-14221-9.
40. Liang, D.; Almeida, J. Solar-Pumped TEM<sub>00</sub> Mode Nd:YAG Laser. *Opt. Express* **2013**, *21*, 25107. [[CrossRef](#)] [[PubMed](#)]
41. Cai, Z.; Zhao, C.; Zhao, Z.; Zhang, J.; Zhang, Z.; Zhang, H. Efficient 38.8 W/m<sup>2</sup> Solar Pumped Laser with a Ce:Nd:YAG Crystal and a Fresnel Lens. *Opt. Express* **2023**, *31*, 1340. [[CrossRef](#)] [[PubMed](#)]
42. Xie, W.T.; Dai, Y.J.; Wang, R.Z.; Sumathy, K. Concentrated Solar Energy Applications Using Fresnel Lenses: A Review. *Renew. Sustain. Energy Rev.* **2011**, *15*, 2588–2606. [[CrossRef](#)]
43. Bernardes, P.H.; Liang, D. Solid-State Laser Pumping by Light Guides. *Appl. Opt.* **2006**, *45*, 3811. [[CrossRef](#)]
44. Vistas, C.R.; Liang, D.; Almeida, J. Solar-Pumped TEM<sub>00</sub> Mode Laser Simple Design with a Grooved Nd:YAG Rod. *Sol. Energy* **2015**, *122*, 1325–1333. [[CrossRef](#)]
45. Zhao, B.; Changming, Z.; He, J.; Yang, S. The Study of Active Medium for Solar-Pumped Solid-State Lasers. *Acta Opt. Sin.* **2007**, *27*, 1797–1801.
46. ASTM G173-03(2012); Standard Tables for Reference Solar Spectral Irradiances: Direct Normal and Hemispherical on 37° Tilted Surface. ASTM International: West Conshohocken, PA, USA, 2020.
47. Prah, S. Nd:YAG–Nd:Y3Al5O12. Available online: <https://omlc.org/spectra/lasermedia/html/052.html> (accessed on 14 March 2023).
48. Dong, J.; Rapaport, A.; Bass, M.; Szpocs, F.; Ueda, K. Temperature-Dependent Stimulated Emission Cross Section and Concentration Quenching in Highly Doped Nd<sup>3+</sup>:YAG Crystals. *Phys. Status Solidi* **2005**, *202*, 2565–2573. [[CrossRef](#)]
49. Almeida, J.; Liang, D.; Vistas, C.R.; Guillot, E. Highly Efficient End-Side-Pumped Nd:YAG Solar Laser by a Heliostat–Parabolic Mirror System. *Appl. Opt.* **2015**, *54*, 1970. [[CrossRef](#)]

50. Liang, D.; Almeida, J.; Vistas, C.R. Scalable Pumping Approach for Extracting the Maximum TEM<sub>00</sub> Solar Laser Power. *Appl. Opt.* **2014**, *53*, 7129. [[CrossRef](#)] [[PubMed](#)]
51. Liang, D.; Almeida, J.; Tibúrcio, B.D.; Catela, M.; Garcia, D.; Costa, H.; Vistas, C.R. Seven-Rod Pumping Approach for the Most Efficient Production of TEM<sub>00</sub> Mode Solar Laser Power by a Fresnel Lens. *J. Sol. Energy Eng.* **2021**, *143*, 061004. [[CrossRef](#)]
52. Tibúrcio, B.D.; Liang, D.; Almeida, J.; Garcia, D.; Catela, M.; Costa, H.; Vistas, C.R. Enhancing TEM<sub>00</sub>-Mode Solar Laser with Beam Merging and Ring-Array Concentrator. *J. Sol. Energy Eng.* **2022**, *144*, 061005. [[CrossRef](#)]

**Disclaimer/Publisher's Note:** The statements, opinions and data contained in all publications are solely those of the individual author(s) and contributor(s) and not of MDPI and/or the editor(s). MDPI and/or the editor(s) disclaim responsibility for any injury to people or property resulting from any ideas, methods, instructions or products referred to in the content.